

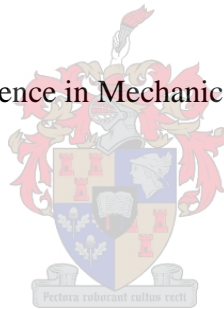
Design, Development and Testing of a 2-DOF Articulated Dump Truck Suspension Seat

by

Charl Barnard

*Thesis at the University of Stellenbosch
in partial fulfilment of the requirements for the
degree of*

Master of Science in Mechanical Engineering



Department of Mechanical and Mechatronic Engineering
Stellenbosch University
Private Bag X1, 7602 Matieland, South Africa

Study Leader: Prof J.L. van Niekerk

October 2008

6. Computer Modelling

6.1 ADAMS modelling

ADAMS was used for modelling the mechanisms to evaluate performance, stability and to give more insight into the mechanisms' behaviour. The mechanism models could only translate in the yz-plane. The ADAMS modelling resulted in the concept to be used for the first prototype design to be changed from the Hex Linkage concept to the Two Part Mechanism concept. See Appendix C for diagrams of the suspension mechanism ADAMS models. A basic air-spring model was used in the ADAMS models. The basic air-spring model was derived from the ideal gas equation. The derivation of the air-spring model is given in Paragraph 6.2.2.

6.2 Matlab Simulink modelling

Numerical and analytical models concerning the suspension seat's vertical movement with a human occupant were run in Matlab Simulink. The purpose of the models was to better understand the dynamic behaviour of the suspension seat's vertical movement and the influence of parameter changes. Two numerical models were completed; an air spring with external reservoir model and a suspension seat with human occupant model. The air spring with external reservoir model was used in the completed vertical suspension with human occupant model. A simplified analytical air spring with external reservoir model to be used in ADAMS was also developed. The model was compared to the numerical air spring with reservoir model in Matlab Simulink and gave good correlation.

6.2.1 Vertical model of human on a suspension seat

Although there are many different models to simulate human response to vibration, a single method to adapt the model to fit the test subject does not exist. Human response to vibration is complicated and depends greatly on inter-subject and intra-subject variability. Inter-subject variability refers to the difference between subjects in aspects such as body mass, size and previous experience. Intra-subject variability refers to changes in the same subject like different body posture and a different reaction to the vibration after being exposed to it before.

Figure 14 shows the lumped parameter model used to simulate the suspension seat with a human occupant. The model was adapted from Wu *et al.* (1999). A lumped parameter model is a model in which each mass is simulated as a point. Mass subscript numbers 0 to 3 represents the human model and mass m_4 represents the total seat and mechanism mass. Subscripts 1 to 3 for spring and damper elements represent the human model, subscript 4 the polyurethane seat and human interaction and subscript s the suspension mechanism. For the human model the mass, stiffness and damping components do not represent any actual part of the human body, as it is a lumped parameter model that fits test data.

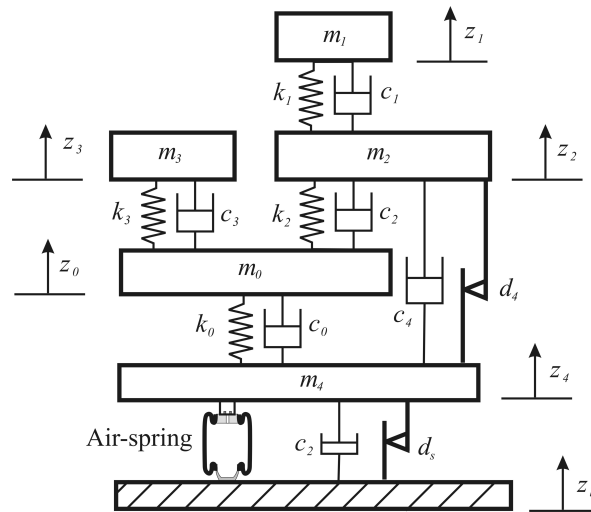


Figure 14: Vertical model of human on suspension seat, solved with Matlab Simulink

Because of subject variability the initial human model used from Wu *et al.* (1999) was modified to fit the test data from the laboratory suspension seat tests. The testing was performed with three human subjects, referred to as the small, medium and large subjects. The parameters for each of these human test subjects had to be determined. The parameters were initially changed to fit the test data for the medium human subject. To determine the parameters for the small and large subjects, a linear relation was assumed between the mass values and the damping and spring coefficients for all the human models. Thus each component for the human model was multiplied by a coefficient that equalled the total mass of the subject divided by the total mass from the medium subject model. This worked to some degree, but parameters still had to be modified further to fit the test data of the small and large subject. See Chapter 6.2.3 for the method used to determine the unknown model parameters. The model parameters used in this research are compared with those found in literature in Table 5, below.

Table 5: Comparison of model parameters to those in literature

Parameter	This project	Gunston <i>et al.</i> (2002)	Wu <i>et al.</i> (1999)
m_0 (kg)	3.5	N/A	3.5
m_1 (kg)	42.6	N/A	42.6
m_2 (kg)	2	N/A	2
m_3 (kg)	5.7	N/A	5.7
m_T (kg)	53.8	58	53.8
m_4 (kg)	39.4	16	10
k_1 (N.m ⁻¹)	31644	N/A	29087
k_2 (N.m ⁻¹)	29087	N/A	45644
k_3 (N.m ⁻¹)	16617	N/A	26617
c_1 (N.s.m ⁻¹)	70	N/A	1305
c_2 (N.s.m ⁻¹)	1350	N/A	1305

Table 5 (continued):

c_3 (N.s.m ⁻¹)	175	N/A	1305
d_s (kg)	120	74	N/A
c_s (N.s.m ⁻¹)	20	N/A	892
k_0 (N.m ⁻¹)	25583	92100	82300
c_0 (N.s.m ⁻¹)	80	1371	300

All the parameters from different sources in Table 5 do not coincide. Gunston *et al.* (2002) modelled the human as a single rigid mass and the model from Wu *et al.* (1999) was modified for this project. Figure 15 compares the modelled data using the parameters from Wu *et al.* (1999) and the modified model from this project to the measured data. The measured data was obtained from vertical suspension seat tests with a human occupant, which will be explained in Chapter 7. The parameters of the original human and seat model from Wu *et al.* (1999) were modified until the modelled data fitted the measured data. The stiffness and damping coefficients were generally decreased. The seat used for this project was from a small vehicle and not an ADT and when comparing the different seats, small vehicles seats are “softer” than ADT seats. This explains why the parameters had to be decreased.

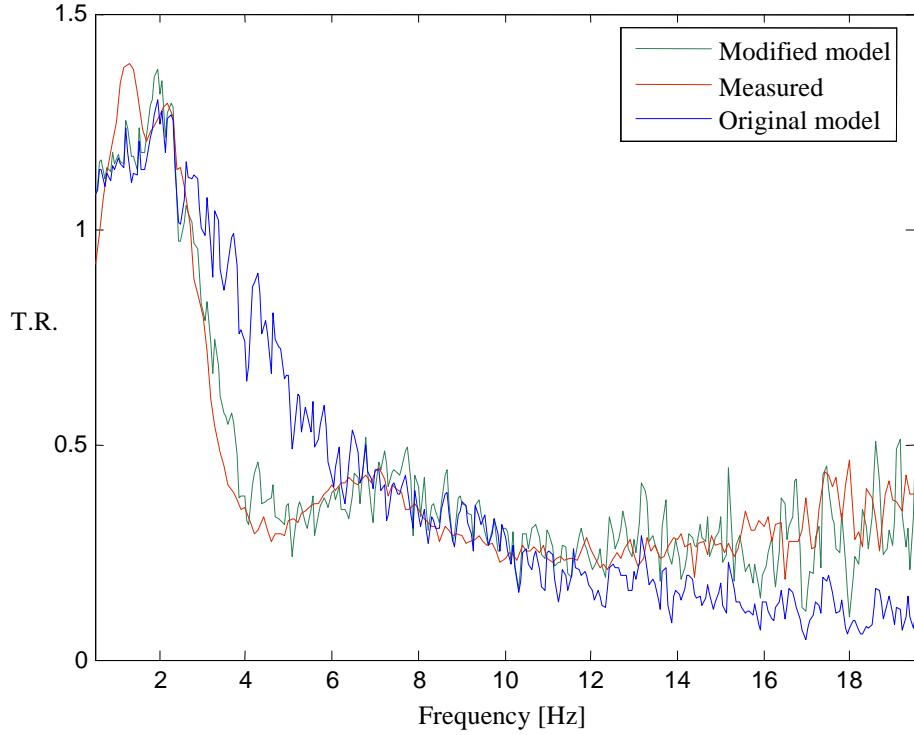


Figure 15: Comparison between original human model from Wu *et al.* (1999) and modified human model to the measured data

6.2.2 Air-spring model

The air spring with external reservoir model was derived from the theory of air flow through an orifice and the ideal gas equation. The equations were solved numerically with Matlab Simulink. The air spring and reservoir are two different sections separated by an orifice. To simplify the model, the temperature inside the air spring and reservoir are taken as constant and equal to the ambient temperature. The system was assumed to be adiabatic. The strategy for modelling the air spring and reservoir was to first model air flow through an orifice with a high pressure section and a lower pressure section downstream. When the air spring is active the high pressure section will alternate between the air spring and reservoir. A detailed derivation of the air-spring model can be found in Appendix A.1.

The temperature was simplified to be constant and the air density was calculated from the high upstream pressure:

$$\rho = \frac{P_1}{RT} \quad (6.1)$$

The mass flow between the air-spring and reservoir is given by:

$$\dot{m} = CA_2 P_1 \sqrt{\frac{2}{RT} \left(\frac{n}{n-1} \right) \left(w^{2/n} - w^{(n+1)/n} \right)} \quad (6.2)$$

With the direction of the mass flow dependent on the pressure difference between the air-spring and reservoir.

The time derivative of the pressure inside the air-spring is:

$$\dot{P}_a = \frac{\dot{m}RT - \dot{V}_a P_a}{V_a} \quad (6.3)$$

The volume of the air-spring (V_a) is dependent on the translation between the base and top of the air-spring.

The time derivative of the pressure inside the air-reservoir is:

$$\dot{P}_r = \frac{\dot{m}RT_r}{V_r} \quad (6.4)$$

The reservoir volume (V_r) is a constant.

The force exerted by the air spring is given by:

$$F_s = (P_{atm} - P_a) A_a \quad (6.5)$$

Equations 6.1 to 6.5 were solved numerically using Matlab Simulink. The Matlab Simulink integrator ODE45 (Dormand-Prince) was used to find the solution.

6.2.3 Lateral movement suspension seat rigid mass model

To simulate the lateral movement of the suspension seat a two degree of freedom lumped parameter model was developed and solved numerically using Simulink. Because of symmetry the suspension mechanism, along with the rigid mass, could be simulated with a half section, as shown in Figure 16.

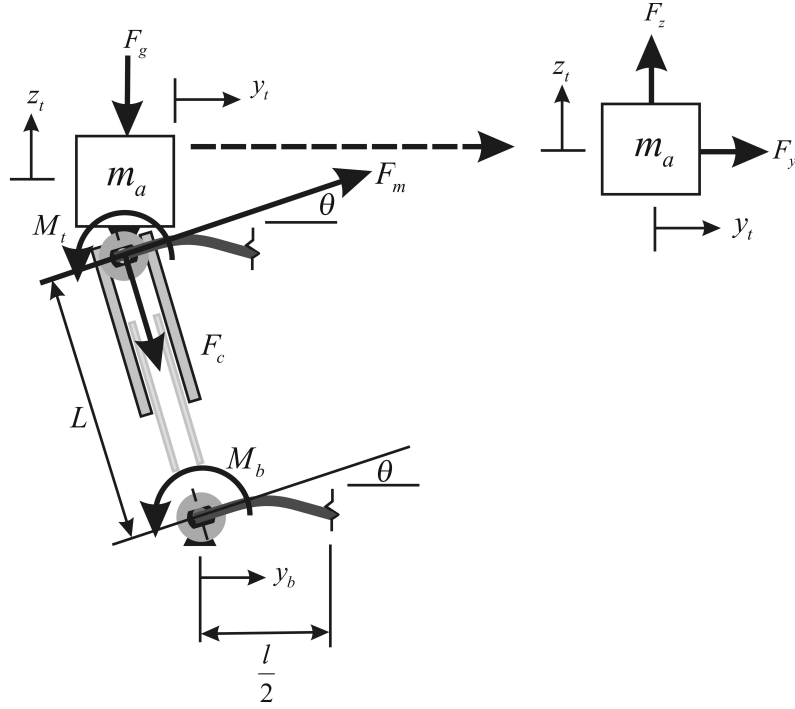


Figure 16: Lumped parameters model of suspension mechanism with rigid mass to simulate lateral movement

The bending of the leaf springs causes moments M_t and M_b which are linearly equivalent to the resulting force F_m . To simplify the model the length L is made a constant. The vertical and lateral suspension seat testing in the laboratory are done independently, thus for the lateral testing the suspension will not translate vertically. In reality L does change when the seat translates laterally, but not enough for it to be relevant to the lateral model. The purpose of the force F_c is to stabilise the model and prevent the length L from changing.

Determining state equations

From Benham *et al.* (1996) the initial gradient θ equals:

$$\theta = \frac{Ml}{4EI} \quad (6.6)$$

Also assuming a linear relationship, the acting moment equals:

$$M = \theta k + \dot{\theta} c \quad (6.7)$$

Thus stiffness and damping coefficients equals:

$$k = \frac{4EI}{l} \quad (6.8)$$

and

$$c = \text{constant} \quad (6.9)$$

This was then applied to the top and bottom leaf springs. The mechanism moments acting on the lumped mass are:

$$M_t = \theta k_t + \dot{\theta} c_t \quad (6.10)$$

$$M_b = \theta k_b + \dot{\theta} c_b \quad (6.11)$$

The force acting on the mass is dependent of both moments:

$$F_m = \frac{(M_t + M_b)}{L} \quad (6.12)$$

$$\therefore F_m = \frac{4E_s(4I_t + I_b)}{Ll} \theta + (c_t + c_b) \dot{\theta} = k_1 \theta + c \dot{\theta} \quad (6.13)$$

with,

$$\theta = \text{atan}\left(\frac{y_b - y_t}{L + z_t}\right) \quad (6.14)$$

The 4 before I_t in Equation 6.41 is a result of the addition of the moments from the top four leaf springs. Each of the top four leaf springs experiences the same angular rotation and thus responds with the same moment.

The force acting on lumped mass (m) because of gravity is:

$$F_g = mg \quad (6.15)$$

Although the arm length (L) does change in reality, it was held constant to simplify the model. Length change of the arms was incorporated in the model for future refinement of the model to incorporate vertical travel. For the model used in this project it was given a high stiffness value to force the length to remain constant.

The acting force from the arms is:

$$F_c = \left[L - \sqrt{\left((y_b - y_t)^2 + (L + z_t)^2 \right)} \right] \times 10^7 \quad (6.16)$$

The lateral acceleration of mass m is:

$$\ddot{y}_t = \frac{1}{m_a} [2F_m \cos(\theta) + F_c \sin(\theta)] \quad (6.17)$$

The vertical acceleration of mass m is:

$$\ddot{z}_t = \frac{1}{m_a} [2F_m \sin(\theta) + F_c \cos(\theta) - F_g] \quad (6.18)$$

Equations 6.45 and 6.46 were solved numerically with Matalb Simulink. Model simulation results are discussed in Paragraph 8.4. The Matlab Simulink integrator ODE45 (Dormand-Prince) was used to find the solution.

6.2.4 Parameter identification program

The vertical mechanism and seat friction are a combination of viscous and coulomb damping. These parameters were determined experimentally with the aid of a parameter identification program. The program uses the Matlab constrained non-linear optimization function *fmincon.m* to identify two parameters for each run by finding the constrained minimum for an objective function. More

parameters could have been identified, but it was not necessary. The objective function that was minimized is the normalized difference between test data and modelled data for a given frequency range. Estimates were used for the initial values and feasible ranges for the boundary values. The program can be applied to Simulink models.

The first set of vertical laboratory testing was done with different number of weights and then from this, using the parameter identification program, the viscous and coulomb damping values of the mechanism were determined. The viscous and coulomb damping values were then determined for the human subject on the seat. Different parameters influenced the fixed frequency ranges. After it was determined which parameters influenced which frequency range the program was used to determine the parameters so that the test and model data fitted. Figure 17 shows the results of the program changing the coulomb and viscous damping values until the model data fits the test data.

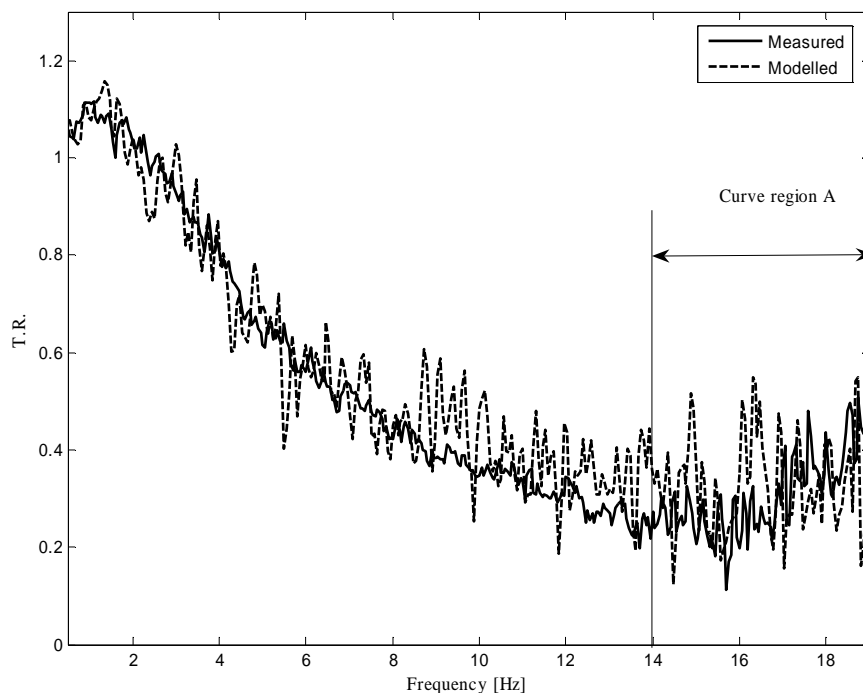


Figure 17: Results of the parameter identification program and the frequency range used for the objective function of the rigid mass tests

Curve region A (as indicated in Figure 17) was used for the parameter identification because it was necessary to determine what caused the positive gradient that started after 14 Hz. The program results showed the coulomb damping value to be relatively large and the viscous damping low, as expected. A higher coulomb damping value in the numerical model resulted in a more distorted PSD plot and a higher viscous damping value caused a smoother plot.

7. Vertical Seat Testing and Evaluation

The vertical and lateral laboratory tests could only be done separately. Equipment to do the vertical seat testing on was available. It was not feasible or safe to modify the equipment for lateral testing as well. A separate test setup for lateral seat testing had to be designed and built. This chapter only focuses on the vertical suspension seat test setup and results.

Three sets of vertical tests were done on the suspension seat. The first set of testing was done with different masses on the suspension mechanism, to determine the transmissibility of the suspension mechanism. A broad band input signal (see Figure 18) was used as base excitation. The same broad band signal was also used for the second set of tests done with human occupants sitting on the polyurethane seat, attached to the suspension mechanism.

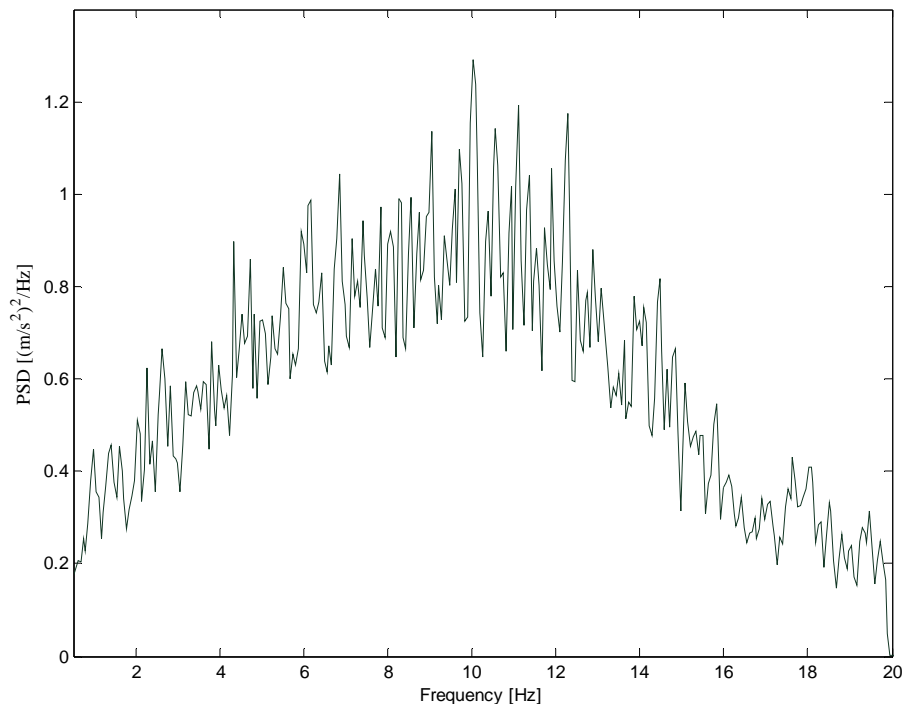


Figure 18: PSD input of base excitation vibration

All the vertical suspension seat testing was performed on the DSTF (Dynamic Seat Testing Facility) in the Structures Laboratory at Stellenbosch University. The DSTF complies with the safety requirements according to ISO 13090-1 (1990) and is safe to use with human test subjects. The DSTF consists of a man-rated single axis platform (z-axis), a servo hydraulic actuator, a safety system and a control system. The suspension mechanism with the seat was attached to the platform. Numerous emergency stop buttons are located around the test setup, easily accessible by the operator and test subject. The servo-hydraulic actuator has a usable stroke of 150 mm and can produce a frequency of up to 25 Hz.

The data acquisition and displacement control was done with a computer using Matlab based software called SigLab. Data was sampled at 51.2 Hz, a low pass filter was used to prevent aliasing and 50 averages were taken of measurements lasting 20 seconds each. Thus every test lasted 16 minutes and 40 seconds.

The third set of required vertical testing to determine the SEAT values of the suspension seat with human occupants could not be done on the DSTF, because the actuator could not produce the required stroke. The numerical model of the suspension seat with human occupant was used to determine the SEAT values. The input signal used was generated from the required PSD signal according to ISO 7096 (2000) EM1. Figure 19 (overleaf) shows the required PSD and the PSD of the generated signal. See Appendix A.2 for the method used to generate the PSD.

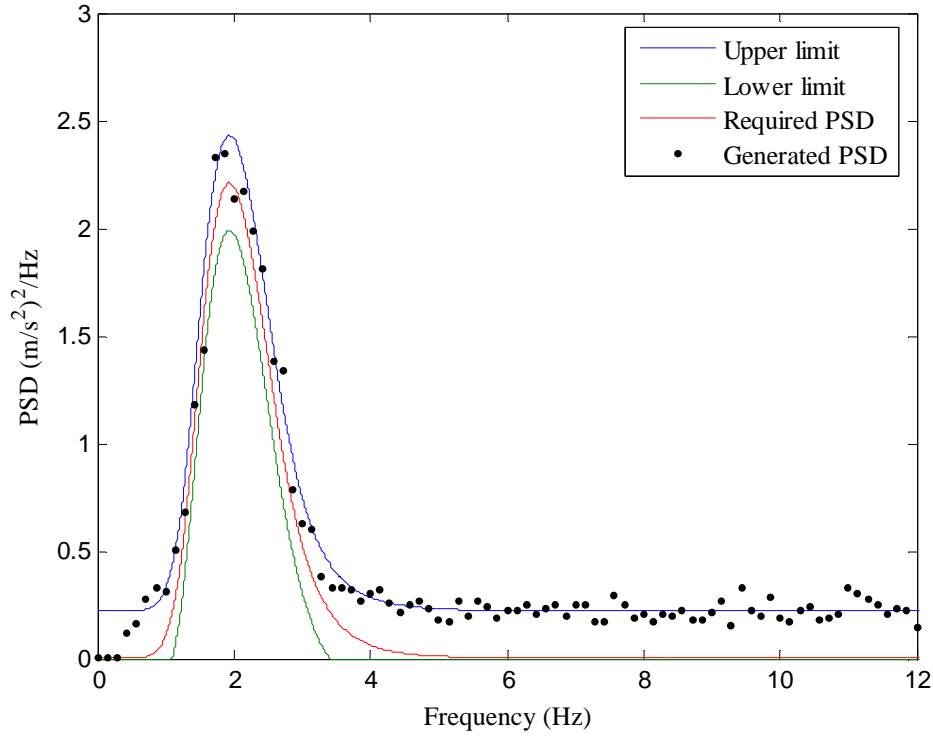


Figure 19: PSD of input vibration of spectral class EM1 according to ISO 7096 (2000)

7.1 Rigid mass test setup and procedure

The main purpose of the rigid mass testing was to verify the air spring with external reservoir model and determine the damping values of the mechanism. The test setup consisted of the suspension mechanism without the polyurethane seat, loaded with 15 kg weights. Figure 20 shows this test setup without the weights.

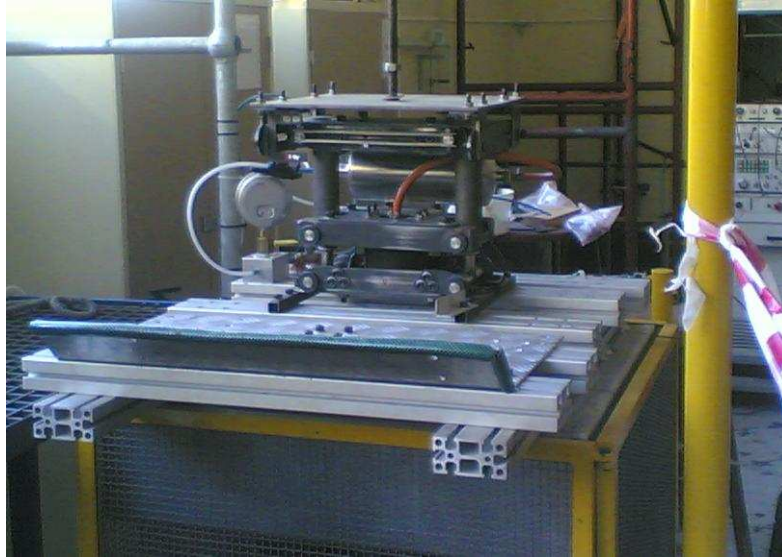


Figure 20: Rigid mass test setup (without weights) on DSTF

Two accelerometers were used to determine the suspension transmissibility, one attached to the actuator platform (PCB Model No. 3701D1FA20G, SN5551) and the other (PCB Model No. 3701D1FA20G, SN7432) to the top moving part of the suspension mechanism above the air spring (as indicated in Figure 20). The transmissibility was determined from the two channels of measured acceleration data for three different loads: 60 kg, 45 kg and 30 kg. The pressure inside the air spring and reservoir was adjusted to compensate for the different masses. To return the air spring to its original height a mechanical pressure measuring device was used. The broad band input signal from Figure 18 was used for the base excitation. To compare the measured pressure difference between the air spring and reservoir to the modelled pressure difference, a pressure transducer calibrated with a Betz manometer was used. The base vibration was set to 3 Hz and the displacement was measured with the displacement meter, calibrated with precision machined metal blocks. The displacement meter data was used in the air spring with external reservoir numerical model and compared to the measured data.

7.2 Human occupant seat test setup and procedure

Three human subjects were used for testing to determine the seat transmissibility ratio plot. All the subjects were informed of their rights and of the adverse effects of whole-body vibration, and all signed consent forms. The subject weights were 71 kg, 84 kg and 94 kg. Figure 7 shows a diagram of the test setup.

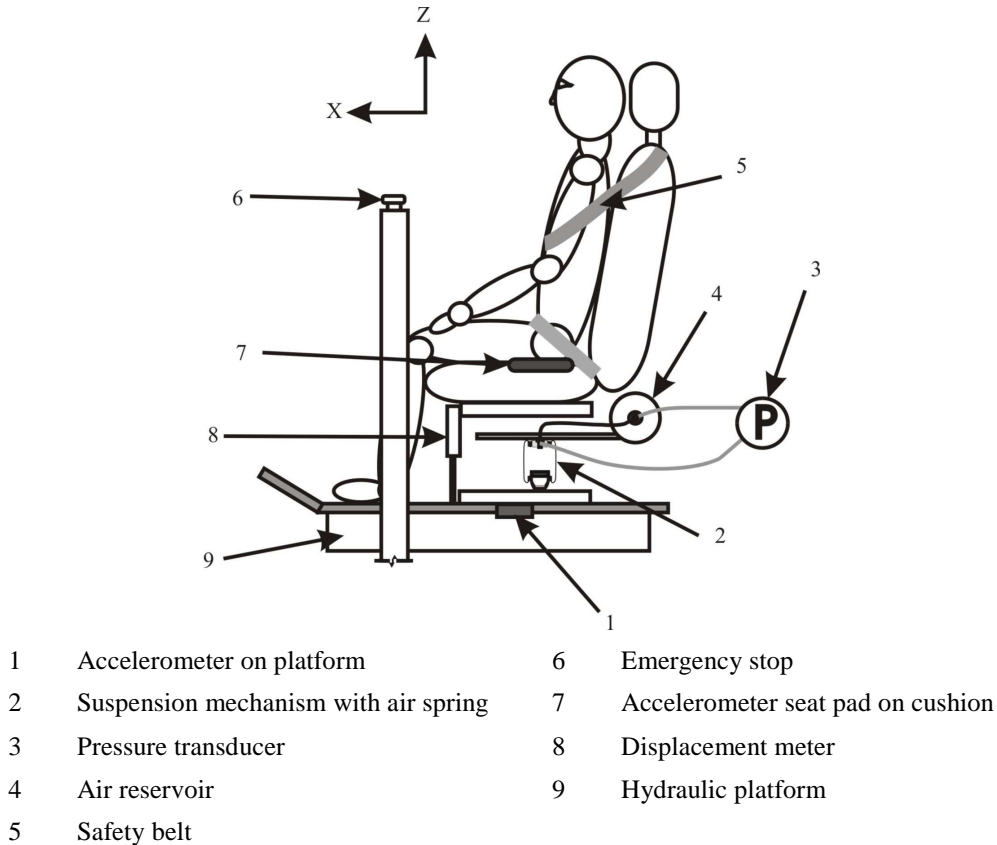


Figure 21: Side view of suspension seat human occupant test setup

Two channels of accelerometer data were used to determine the transmissibility ratio. A PCB Piezotronics seat pad with a tri-axial accelerometer (Model No. 356B40) was used on the seat surface, approximately 120 mm from the seatback. The seat pad was taped to the seat surface. The base excitation vibration was measured using a Piezotronics single axis accelerometer (Model No. 3701D1FA20G, SN 7432), secured by screw point.

7.3 Vertical test results

7.3.1 Rigid mass tests

Figure 22 shows the test results for the rigid mass tests. The plot shows the same trend as would normally be expected from a 1-dof spring-damper-mass system being exposed to base excitation. The system amplifies vibration below approximately 2 Hz and isolates it above 2 Hz. At resonance the transmissibility ratio does not go above 1.2 which is mainly due to the inherent damping in the mechanism and the pressure difference between the air spring and reservoir.

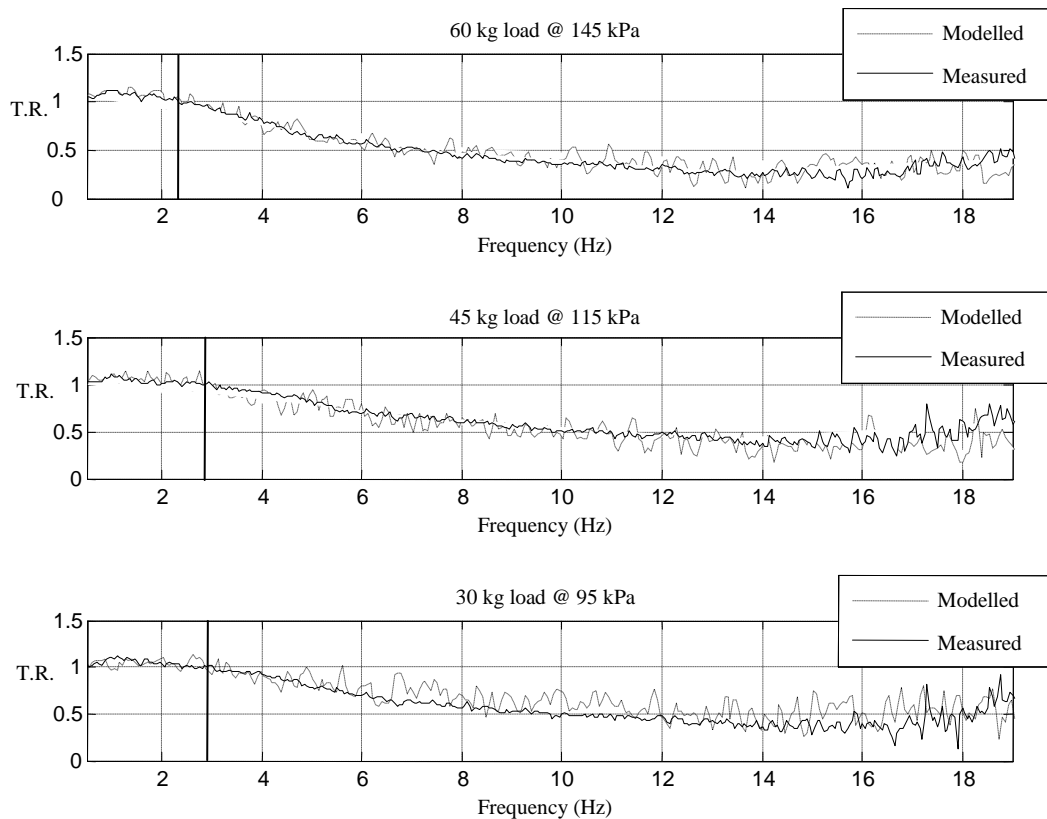


Figure 22: Transmissibility ratios vs. frequency of suspension mechanisms

The resonance frequency for every weight setup is approximately 1.4 Hz. Unlike a normal coil spring the air-spring maintains the same natural frequency independent of the acting mass. The air-spring must be used in its recommended

operating range. Unlike the frictional coulomb damping of the mechanism, the damping caused by the air spring and reservoir can be modelled and determined without prior testing. Figure 23 shows the pressure difference measured and modelled and confirms that the air spring with external reservoir numerical model does give an accurate representation of the air spring damping.

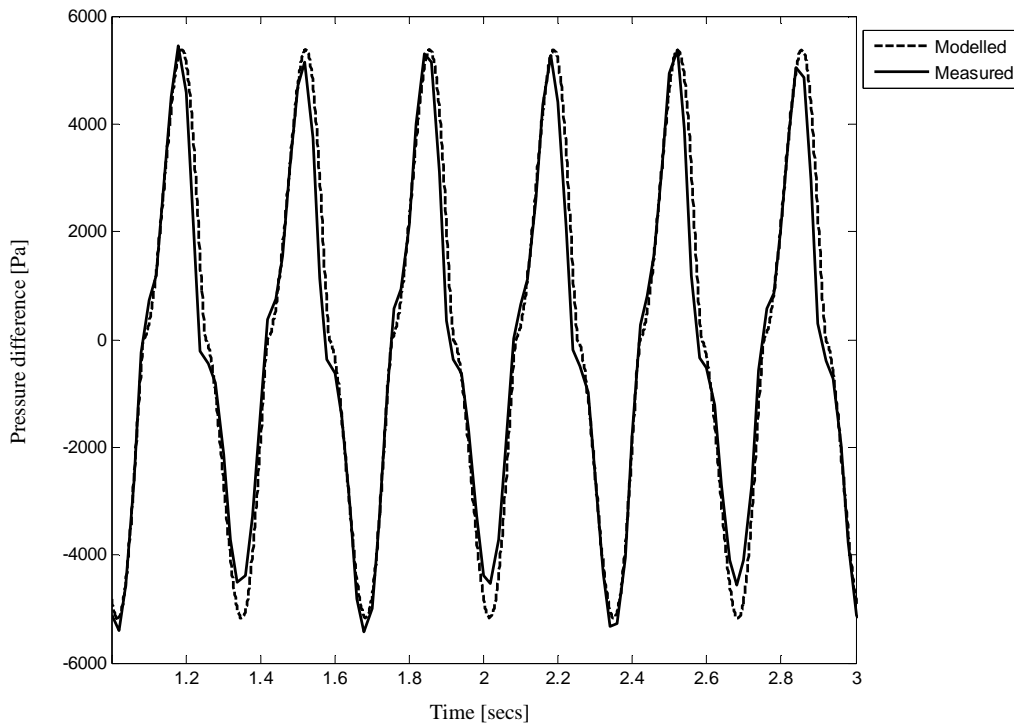


Figure 23: Pressure difference between air spring and external reservoir

The system identification algorithm was used to identify the viscous and coulomb damping values. The values were determined with data from each of the three rigid mass tests. As can be seen from Table 6, the values do not completely coincide, but an averaged value does give good approximated results.

Table 6: Damping values determined by variable identification algorithm

Weight mass [kg]	Coulomb damping value [N]	Viscous damping value [N.s/m]
30	113	643
45	125	730
60	110	652
Average	117	675

Between 14 Hz and 20 Hz the transmissibility ratio starts to increase slightly again. When the algorithm was programmed to identify the damping values for curve fitting below 14 Hz the modelled data followed the trend of the measured data below but not after 14 Hz. When the algorithm determined the damping values using values between 14 Hz and 20 Hz the trends of the measured and modelled data fitted satisfactorily for the entire relevant frequency range (0.5 Hz to 20 Hz).

7.3.2 Human occupant seat testing

The dynamic behaviour of the suspension seat with a human occupant can be evaluated from the transmissibility graphs. The numerical model was used to identify and explain the different behavioural trends of the transmissibility graphs. With the mechanism and air spring model parameters identified from the rigid mass tests, the complete human occupant on suspension seat model was modified to fit the test data.

When evaluating all the transmissibility graphs showing the results from the human occupant suspension seat testing there is approximately a 1.4 Hz resonance peak in all the graphs (see Figure 24, Figure 25 and Figure 26). This is most likely caused by the air spring with external reservoir, as was observed with the rigid mass tests. It was decided that the seat occupant on the polyurethane foam cushion caused the next peak at approximately 2.5 Hz. To cause a peak at such a low frequency a fairly high mass with low stiffness is required. The only other

possibility was the seat's backrest, but it was too rigid and did not translate enough. Thus it could only have been caused by the seat's occupant. The seat's cushion damping and stiffness values were modified to fit the peak at 2.5 Hz.

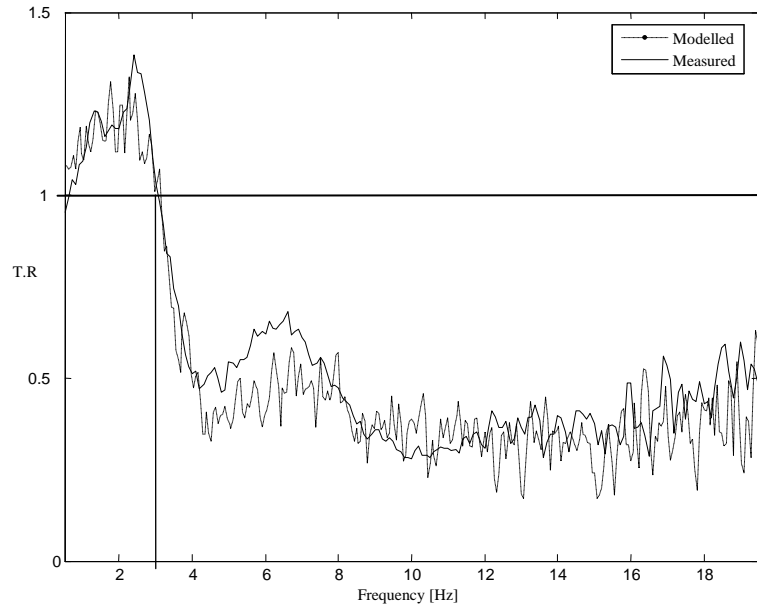


Figure 24: Transmissibility in the vertical direction of small subject

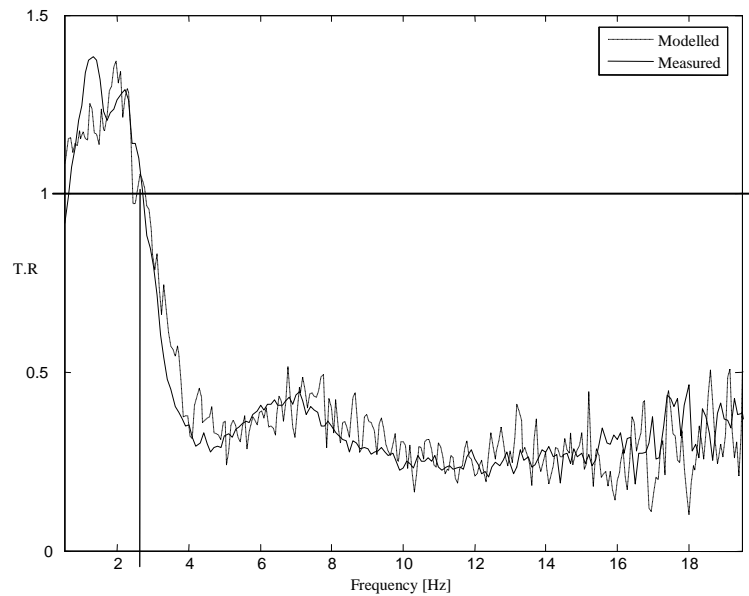


Figure 25: Transmissibility in the vertical direction of medium subject

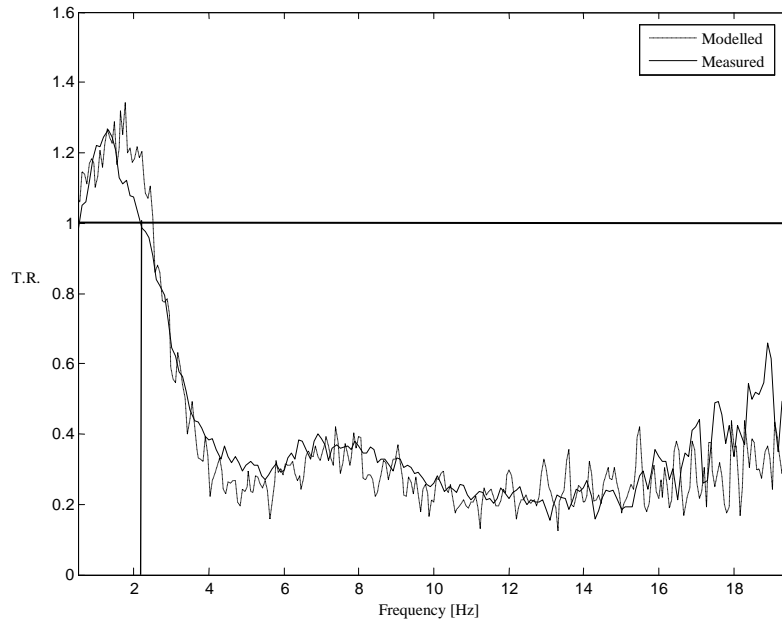


Figure 26: Transmissibility in the vertical direction of large subject

The next two dips on the graph were caused by the translation of the seat's occupant on the seat. The damping and stiffness values of the person were also modified to fit the measured data curve. The first dip was caused by the translation of the person's upper body and the second dip by the translation of the upper legs. To greatly simplify the models, linear behaviour for the seat cushion and human models was assumed.

The acting weight of the person sitting on the seat was determined by measuring the pressure inside the air spring and reservoir. The same weight ratios of each mass relative to the total mass of the human model were used for all the subjects. The original mass, stiffness and damping values were obtained from Wu *et al.* (1999) and modified to fit the medium subject's measured data. The numerical model was first made to fit the test data of the medium subject.

The mass ratio values were determined by dividing the acting mass of the small and large subject by the medium subject's acting mass:

$$h_s = \frac{m_H(\text{small subject})}{m_H(\text{medium subject})} \quad (7.1)$$

$$h_l = \frac{m_H(\text{large subject})}{m_H(\text{medium subject})} \quad (7.2)$$

The acting mass was obtained with the pressure measurements inside the air-spring. With the air-spring's effective diameter known the seat occupant's acting mass could be determined. The medium subject's mass ratio value is unity. Assuming that the total mass of the subject influences the stiffness and damping values of the human model, the parameters of the small and large subjects were multiplied by the mass ratio value, to determine the new parameters for each of the human models.

The only other value that was further modified for the small and large subjects was the cushion damping value to obtain the same peak value at 2.5 Hz.

The only variables that were changed for each subject were the acting mass, pressure inside the air-spring and friction damping value d_4 . The other variables were the same for each subject.

7.3.3 Suspension seat performance

The purpose of the SEAT value is to compare the performance of different suspension seats in a laboratory. Estimated SEAT values were obtained from Gunaselvam (2004). The suspension seat numerical models were used to determine the SEAT values, rather than the laboratory testing as recommended by ISO EM1 as the DSTF actuator does not have the required vertical stroke to produce the ISO EM1 signal displacement. The SEAT values obtained from the numerical models are given in Table 7.

Table 7: SEAT values obtained from numerical models with EM1 signal input.

	Subject		
	Small (68 kg)	Medium (76 kg)	Large (94 kg)
SEAT value	0.94	0.93	0.88

The laboratory testing would have been more accurate than using the numerical models, but using the numerical models are still more accurate than computing the SEAT values with seat transmissibility data, as was done by Gunaselvam (2004). This method would have been fairly accurate if the suspension seat demonstrated linear behaviour. Gunaselvam (2004) estimated the SEAT values with only heavy subjects weighing 94 kg, 91.2 kg and 94.1 kg. Thus the SEAT values from Gunaselvam (2004) can only be compared to this project's heavy subject (94kg).

Gunaselvam (2004) determined the SEAT values for six different suspension seats with three large subjects (98 kg – 103 kg). The best SEAT value obtained was 0.85. The seat with the SEAT value of 0.85 had a similar transmissibility ratio plot to this project's new suspension seat, with the new seat having a slightly lower resonance, approximately the same peak value and a similar end transmissibility.

The numerical suspension seat models were also used with the Bell ADT cabin vibration data to determine the vibration level reduction ratio, the weighted rms value measured above the seat divided by the weighted base rms value. This is the same as the SEAT value, but named differently because the required EM1 signal was not used as the base input. The value indicates the percentage of the vibration experienced by the seat occupant. These values are summarised in Table 8, where the weighted rms value on the seat surface and its percentage of the base vibration are given.

Table 8: Modelled vibration exposure of suspension seat occupant from ADT cabin vibration data

Data file #	Road condition according to Bell log book	Small subject		Medium subject		Large subject	
		rms [m.s ⁻²]	SEAT	rms [m.s ⁻²]	SEAT	rms [m.s ⁻²]	SEAT
4	Medium gravel	1.08	0.63	0.97	0.56	0.83	0.48
22	Bad gravel	1.25	0.65	1.16	0.60	1.03	0.53
27	Medium gravel	0.81	0.73	0.74	0.66	0.63	0.57
31	Standing still	0.39	0.88	0.36	0.81	0.31	0.70
53	Graded gravel	0.91	0.74	0.84	0.69	0.74	0.61
62	Tar road	0.36	1.10	0.34	1.02	0.29	0.88

The suspension seat only amplifies vibration when driving on a tar road (data file 62) and exceeds the recommended vibration limit for an 8-hour day for the small and medium subject when the ADT is driving on a bad gravel road (data file 22). The results are only for vibration in the z-axis and do not take into consideration the weighted rms values of the other axes.

7.4 Vertical testing conclusions

The new ADT suspension seat reduces vibration levels considerably and its performance is comparable to the best performance suspension seat that was commercially available in 2006. The new seat has a slightly higher SEAT value than the other suspension seats tested by Gunaselvam (2004); this may be as a result of the heavier test subjects used by Gunaselvam (2004). The new suspension seat reduces vibration levels considerably, but only reduces the vibration level to below the allowable daily exposure level for the large subject.

During the vertical testing the seat was stable and did not at any time threaten the subject's safety.

8. Lateral Suspension Seat Testing

8.1 Experimental setup

A new test setup had to be designed and built for the lateral suspension seat testing. A hydraulic actuator was used to provide lateral motion. The test setup consisted of a roller platform that moves laterally on tracks. The suspension mechanism and hydraulic actuator were bolted to the platform. The tracks were welded onto a square plate that was bolted to the floor.

The actuator could be controlled with a PID to some degree, but not accurately enough to follow a required input signal, because the response from the controller was too slow. Thus the control was done manually. Piezotronics single axis accelerometers were attached to the lateral moving platform (Model No. 3701D1FA20G, SN5551). The base accelerometer was used to determine actual response of the input signal. A signal generator, providing a sine wave, was used for actuator motion input. The platform's lateral acceleration response was monitored with Labview and the frequency value from the signal generator was adjusted until the required frequency was obtained.

For the rigid mass testing and human seat occupant testing the lateral rms values were measured on the platform and above the suspension mechanism. A single frequency sine signal was used for the actuator input signal. To obtain the transmissibility ratio plots the un-weighted rms value above the mechanism was divided by the rms value measured on the platform for different frequencies.

8.2 Rigid mass lateral test setup

Like the vertical test setup loaded with rigid mass, combinations of 15 kg weights were used. The suspension mechanism was loaded with rigid masses of 30 kg, 45 kg and 60 kg. For each load a transmissibility ratio plot was determined. The

reason for testing with rigid weights was to check the safety and stability of the mechanism before human testing, to evaluate the accuracy of the numerical model and to determine the damping coefficients. The lateral test setup is shown in Figure 27. Piezotronics single axis accelerometers were attached to the top of the suspension mechanism (Model No. 3701D1FA20G, SN7432).

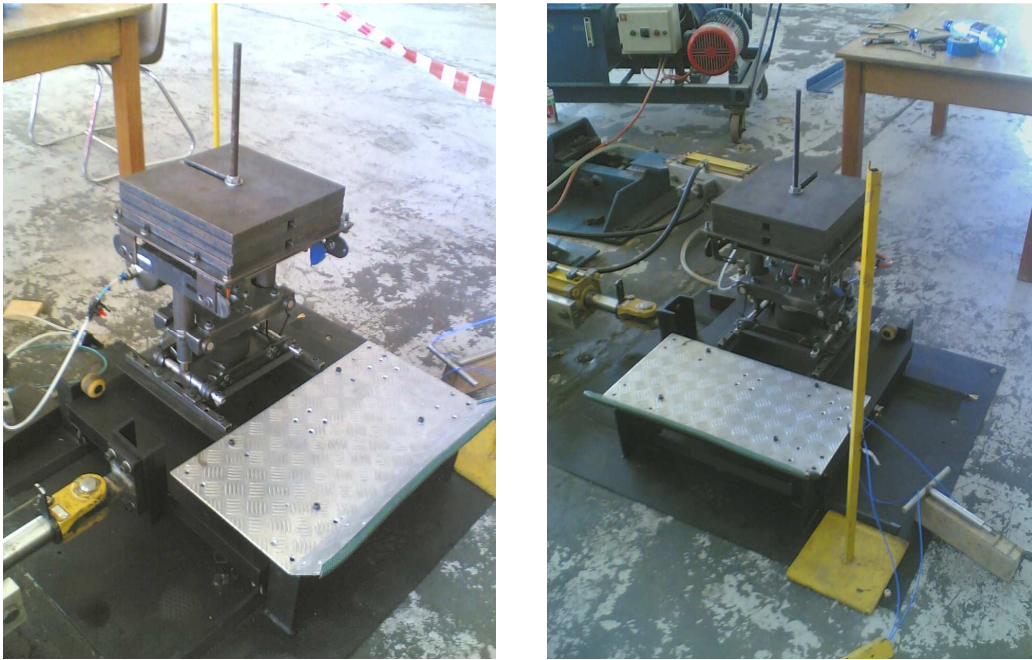


Figure 27: Rigid mass laboratory test setup

8.3 Human seat occupant lateral test setup

The same three subjects used for the vertical tests were used for the lateral tests. As safety was a major concern for the lateral testing, the test subjects were briefed on potential risks and had to sign a consent form. The moving platform was designed not to pose any risk to the human test subject so it was not possible for the subject to get pinched or hit by the moving platform. As a further precaution the hydraulic fluid pressure was set to a value where the actuator movement was not fast enough to cause a person, standing on the platform, to lose their footing.

A PCB Piezotronics seat pad with a tri-axial accelerometer (Model No. 356B40) was used on the seat surface to measure the lateral acceleration. Data from the seat pad and the accelerometer attached to the platform was used to determine the transmissibility plots. Three subjects were used in the testing, a small, medium and large subject. The lateral test setup with a human test subject is illustrated diagrammatically in Figure 28.

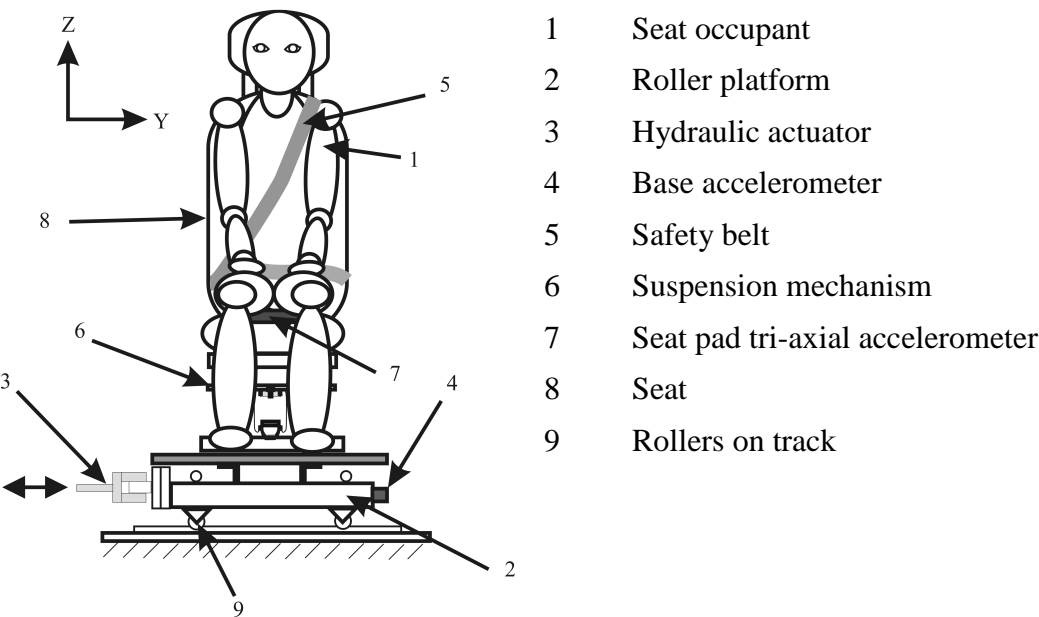


Figure 28: Lateral laboratory test setup for seated human

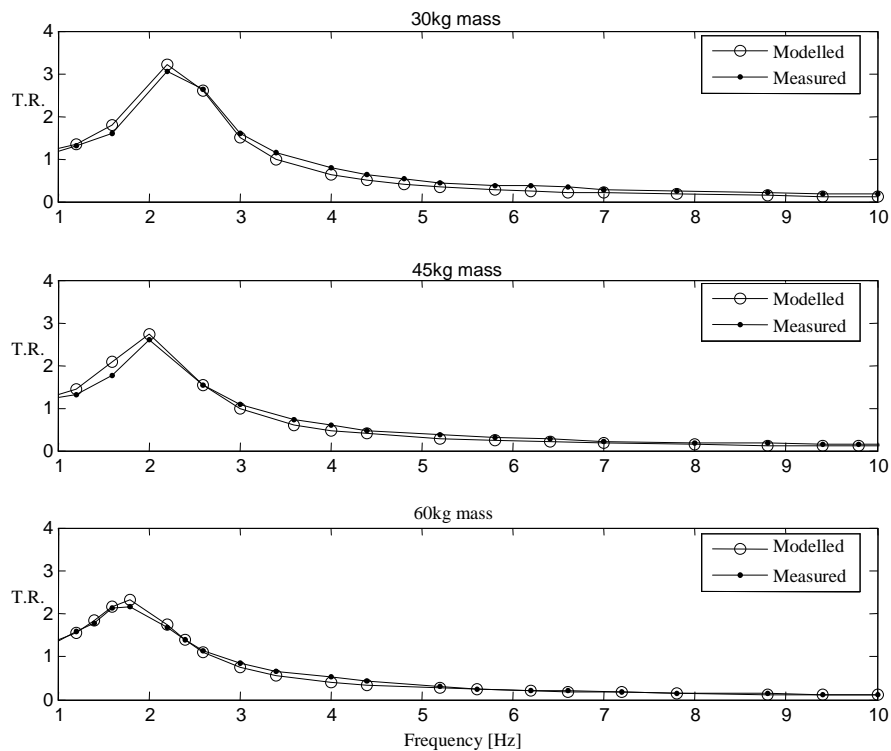
8.4 Rigid mass lateral testing results

The modelled and measured data for the rigid mass tests coincide very closely. The viscous damping values of the numerical models were modified for each weight configuration, to fit the test data. Table 9 shows the mechanism damping values for different acting masses. There are not enough data points for curve fitting to be performed so the only conclusion drawn is that the damping value increases with an increase in the acting mass.

Table 9: Mechanism damping values of lateral numerical model

Mass (kg)	30	45	60
Viscous damping value (N.m.s/rad)	24	34	46

Using viscous damping in the numerical model instead of coulomb damping gave better correlation between the modelled and measured values. As expected the system's natural frequency decreases with the increase of acting mass (see Figure 29). Also with more mass pressing the steel shafts against the Vesconite bushes, the damping values are increased, thus decreasing the transmissibility peak.

**Figure 29: Measured and modelled transmissibility ratios for lateral test setup with rigid masses**

8.5 Human occupant lateral seat testing results

It was found that the human vibration response for lateral excitation is far more complicated than vertical excitation. There are basic three-degrees-of-freedom lumped parameter models (Mansfield *et al.*, 1999) for humans exposed to lateral vibration, but these models did not give good results when fitted against the test data, unlike the vertical model data. The inter-subject variability for the lateral testing also far exceeds that of the vertical testing. Thus the lateral numerical models were not used in this project to evaluate the lateral suspension performance. Rather the measured transmissibility ratios were used.

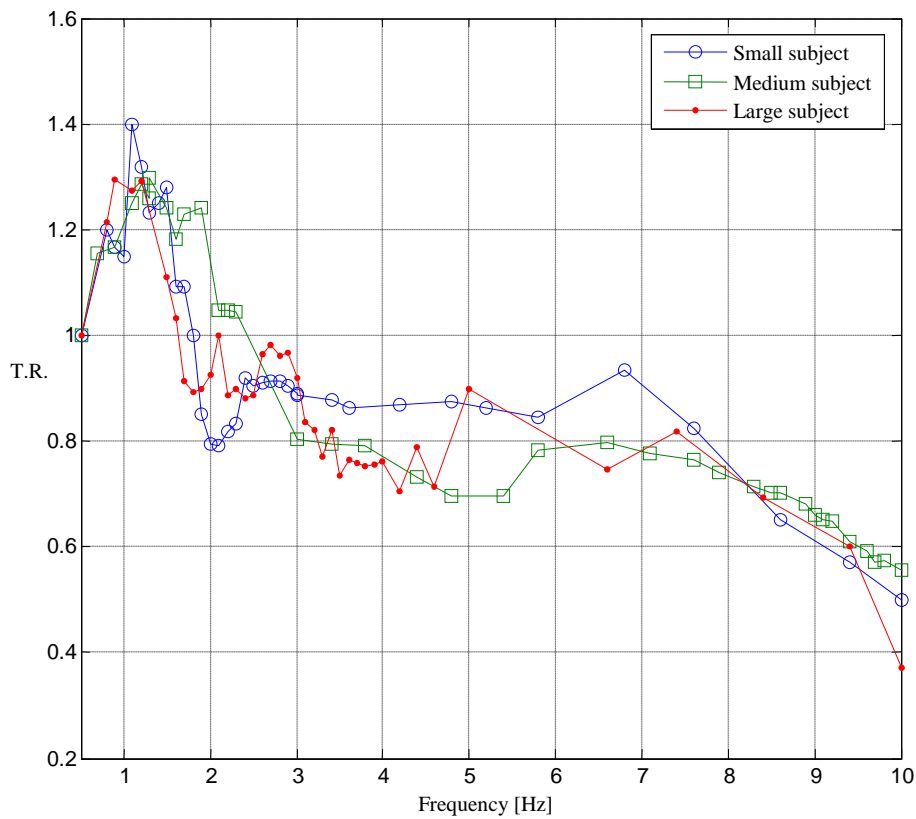


Figure 30: Lateral suspension seat with human occupant test results

As can be seen from Figure 30 there is a general trend amongst all the test subjects, with a peak at approximately 1.4 Hz and a negative gradient after 7 Hz.

Between 1.4 Hz and 7 Hz there is very little correlation between the test data, with no trends that are present for every subject. Thus it can be concluded that with very soft suspension, 1.4 Hz natural frequency, the intra-subject variability is very apparent. It was observed that the suspension seat was more effective at vibration isolation when the subjects lifted up their feet and basically acted as a rigid mass. It was not practical to perform tests with each subject lifting up their feet to determine a transmissibility ratio plot as that is not how a seat is used.

The transmissibility ratios for each subject were used with the ADT data to determine the performance and effectiveness of the lateral suspension system. To determine the PSD at the seat surface, the frequency weighted PSDs of the ADT cabin data were multiplied with the transmissibility ratios from the human lateral seat tests. The weighted rms values on the seat could then be calculated from the PSDs to evaluate the lateral suspension performance, as shown in Table 10.

Table 10: Estimated weighted rms values on seat surface, calculated from lateral T.R. and ADT cabin data

Data file #	Road condition according to Bell log book	Base	Small subject		Medium subject		Large subject	
		rms [m.s ⁻²]	rms [m.s ⁻²]	SEAT	rms [m.s ⁻²]	SEAT	rms [m.s ⁻²]	SEAT
4	Medium gravel	0.72	0.49	0.83	0.59	0.83	0.59	0.82
22	Bad gravel	0.88	0.74	0.85	0.74	0.84	0.74	0.84
27	Medium gravel	0.49	0.43	0.88	0.42	0.87	0.43	0.87
31	Standing still	0.19	0.17	0.93	0.17	0.90	0.17	0.89
53	Graded gravel	0.47	0.40	0.84	0.39	0.84	0.39	0.83
62	Tar road	0.098	0.092	0.94	0.088	0.90	0.088	0.89

Note: The multiplying factor k (1.4) was not applied to the data.

The lateral suspension does reduce the whole body vibration levels. The lateral suspension transmissibility data could only be obtained up to 10 Hz, because of the hydraulic actuator control. The base rms values were only calculated up to 10 Hz. All the transmissibility curves have steep decline before 10 Hz and

because of the low system natural frequency, will not have resonances after 10 Hz. Thus it is likely that if the values in Table 10 were calculated up to 20 Hz, the rms values would have been lower. The possible reduction in the values cannot be estimated with the data available at this stage.

8.6 Lateral testing conclusions

The lateral suspension has a lower natural frequency than the first peak of the measured ADT cabin vibration and should show considerable vibration isolation, but vibration isolation effectiveness gets considerably reduced by the vibration being transmitted through the seat occupant's feet and legs. This effect is clear when comparing the transmissibility ratio plots of the rigid mass test and human tests. The lateral suspension cannot be compared to that of other suspension seats as there are currently no commercial suspension seats available that can reduce lateral vibration or standard test methods (e.g. ISO 2631-1, 1997) for evaluating it. Work done by Greenberg *et al.* (1998) showed the natural frequencies of normal foam seats to be about 4 Hz. With the ADT cabin having a peak at 3 Hz and looking at the foam seats' transmissibility ratios, it can be assumed that the foam seats will amplify the vibration levels. The maximum lateral vibration value measurement found in literature was obtained from Kirstein (2005) and had a value of 1.25 m.s^{-2} . When considering the vibration reduction values from Table 10 the suspension should be able to reduce this value to a maximum of 1 m.s^{-2} , which is below the daily exposure limit. Thus with current cabin vibration data the suspension seat will be able to reduce lateral vibration to recommended safe levels.

9. Technical Assessment

9.1 Design review

A design review of the suspension seat was held, with the purpose to discuss the seat in general, as well as evaluate performance, manufacturability, alternative sub-concepts and improvements for a possible next prototype.

Conclusions from the review which should be considered for a next prototype:

- The $\pm 5^\circ$ rotation around the x-axis must be eliminated, for it will tilt the seat's occupant when the ADT drives at an angle along an incline. It is possible that angular suspension can be incorporated in the design, which will improve ride comfort.
- The concept to use the sliders as viscous or pneumatic dampers is flawed, for the seals will most likely fail before the required ADT's service period. Also one of the customer requirements was not to use any oil damper.
- The use of Rosta units in the design should be re-evaluated. The Rosta unit only gives torsion after approximately 5° , but two Rosta units in pretension acting against each other will initially provide stiffness.
- There are sharp edges on the prototype, which should not be present in upcoming designs.

From the design review it was also concluded that the new suspension seat design does show promise and development of another prototype is justified. The design is original, feasible and differs from the commonly used scissor mechanism.

9.2 Next prototype design

With the information obtained from evaluating and testing the first prototype, another prototype was designed. For this project, because of cost and time constraints, the new prototype was not manufactured. The basic concept from the first prototype still remains, the design was only refined. The redesign was focused on using cost efficient manufacturing techniques, obtaining required tolerances, aesthetic appeal, compact design and further reducing the undesired roll motion.

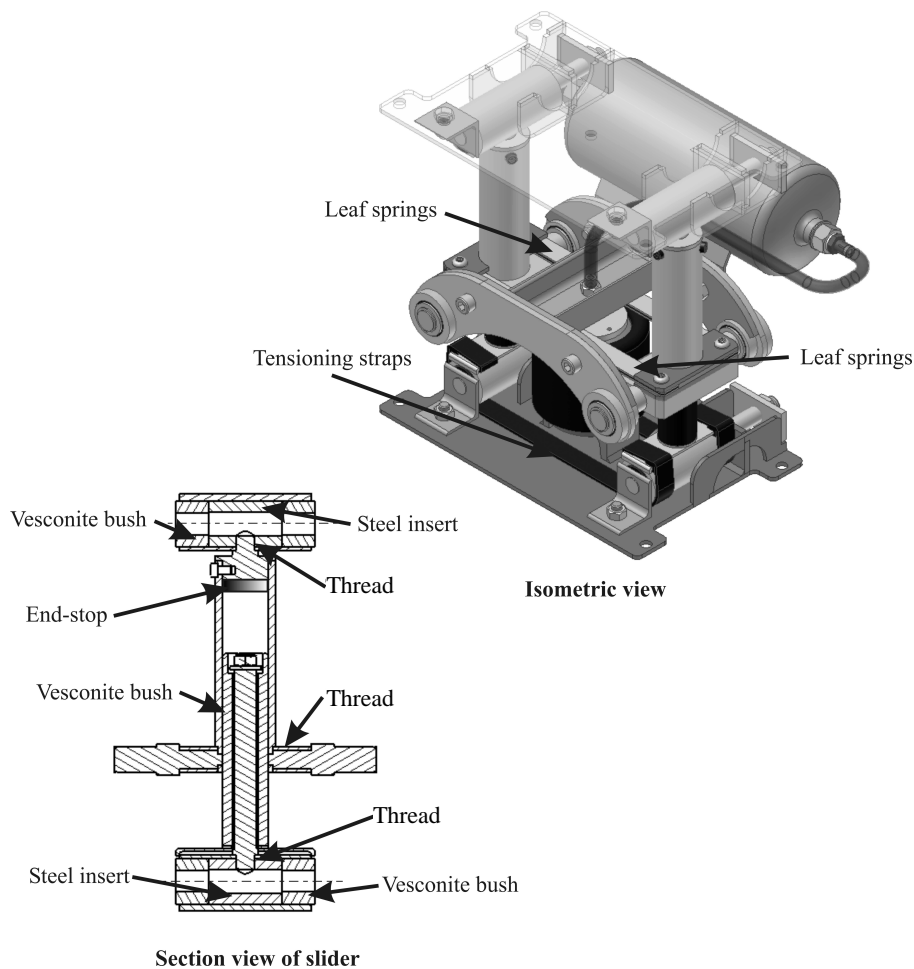


Figure 31: New lateral suspension seat prototype

The vertical slider mechanisms were modified so that the horizontal shafts that use to rotate within the bushes are fixed and now the bushes rotate around the shafts. This allows for the sliders to be removed as a unit with all the components that experiences friction during normal suspension seat operations. The used slider unit can then be completely replaced and the old unit's friction components replaced for re-use on other suspension seat. Another justification for the modification is that it allows the sliders to be manufactured without the use of any welding to minimize unwanted deformation. The sliders are fastened together with machined threads and bolts that will have to be properly torqued to prevent loosening during operation. A tubular steel insert is used in the horizontal slider which acts as a nut for the vertical sliders to screw into.

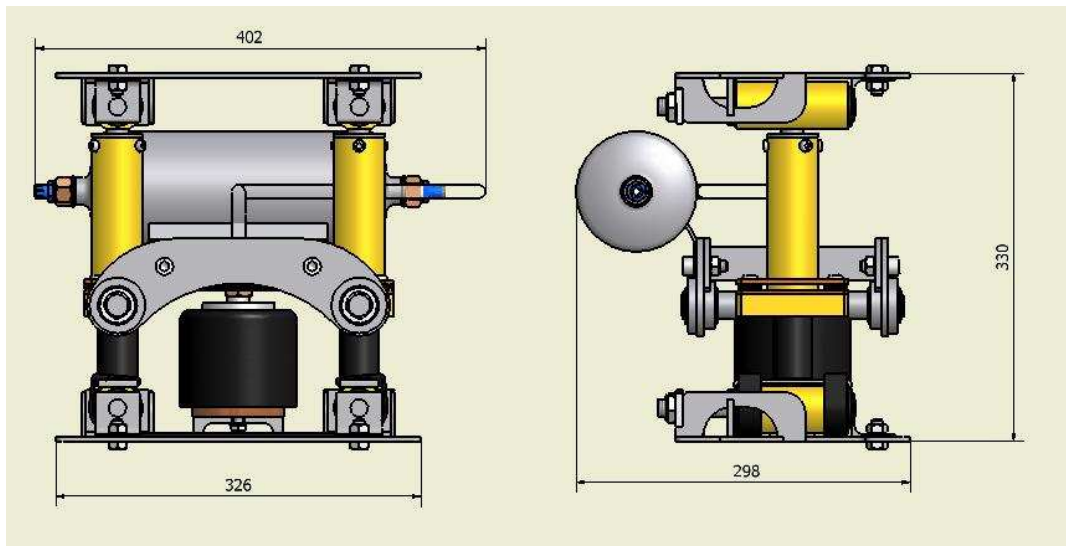


Figure 32: Dimensions of new prototype

The dimensions of the new prototype are 298×402×330 mm . The mechanism will fit under the ADT seat in the cabin. Mechanism mass is 19 kg which was derived from the Inventor solid models.

To reduce the rolling motion that was observed from the first prototype, three design modifications were specifically made:

1. The problem (Paragraph 5.2) was that the bottom parts of the vertical sliders would not remain parallel to each other, instead the angle between them decreased. The tensioning straps will prevent this by pulling the vertical slider apart.
2. The distance which the inner bush slides within the slider have been maximised.
3. To maintain tolerances there are no drilled holes in the hydraulic tubing (outer section of slider).

9.3 Type A specifications review

At the end of every design phase the achievability and feasibility of the specifications must be re-considered. Not all the specifications can be achieved in the first design phases. As the environment and design is better understood, as the project progresses, it becomes evident that some specifications were unrealistic at the start of the project. The following are specifications that have not been met or still needs to be proven:

Performance

1. A suspension seat alone will not be enough to reduce the vibration levels enough for compliance with the EU Directive 2002/44/EC. The new suspension seat did have performance comparable to a high-end commercially available suspension seat. There is a practical limit to how much a suspension seat can reduce low-frequency vibration levels.

Safety and health risks:

- 4 The seat must still be tested to determine if it is strong enough to safely protect the driver in the event of a frontal collision..

Size and weight

1. The weight of the new prototype mechanism is 19 kg, thus the seating must weigh less than 41 kg.

Maintenance

1. The seat can withstand the use of contaminant fluids.
2. The maintenance period of the mechanism in operation has not been determined.
4. No corrosion resistant coatings have yet been specified.

Manufacturing and Cost

1. A complete cost estimation still needs to be done to determine if manufacturing, assembly and packaging costs are below R8 000.

9.4 Future research and testing

This project is still in the preliminary design phase where the technology still has to be evaluated, proven and refined. Studies that still need to be completed relative to this project include the study of different materials to be used for the end-stops and also the bushes, different applicable joining methods and a control system for the pneumatics. Closed-cell polyurethane foam was used for the first prototype's end-stops, but never during the entire laboratory vertical testing were the end-stops ever active. Even with the suspension loaded with a mass of 60 kg and excited at its resonance frequency during laboratory testing. The bushes are made from Vesconite which according to the supplier is a self-lubricating, wear resistant material with a friction coefficient of 0.12 - 0.2 (Vesconite Specifications, 2008). The Vesconite was chosen from specifications obtained from its web-site and information obtained from experienced technicians. Although the material did not show any wear after the laboratory tests, the wear from long term use is unknown and should still be determined. The first two prototypes can easily be modified. The whole mechanism can be disassembled, as it is fastened together with screw-in threaded parts and fasteners. Future suspension seats designed for production will have to be joined with adhesives, press fits, brazing or welding. After a literature search it was concluded that brazing would be the preferred method to mechanically join different components that does not require high strength bonding. Brazing is done at approximately

650°C and welding at 3100°C. Although the welding is more localised the brazing will cause less deformation because it is done at a lower temperature.

Further research must still be completed concerning fore-aft vibration isolation. Rail guided fore-aft suspension is a safety risk in the event of a frontal collision and should not be included. An extensive relevant literature search was completed in the beginning of this project. No information could be obtained explaining the use of different seating positions and cushion materials in trying to reduce fore-aft vibration. There is relevant literature focused on seat cushions, but with the goal of reducing vertical vibration and distributing load. A detailed study evaluating the use of seat cushions in reducing fore-aft vibration may result in a basic, cost-effective and safe solution for reducing fore-aft vibration levels. The lateral test setup designed and manufactured in this project can be used for the research.

A suspension seat alone will not be able to reduce vibration levels within a safe region. Considering a suspension seat also causes drivers to drive recklessly, a vehicle monitoring system is required. This might seem out of the scope of the project, but the project's ultimate goal is to reduce whole-body vibration. With a vehicle monitoring system drivers will be forced to drive safely and in conjunction with a suspension seat will reduce whole body-vibration within the acceptable safety limits. This will reduce the risk of damage to the ADT and also reduce daily production, but the driver's safety from vibration will be guaranteed.

10. Conclusions and Recommendations

A safe working environment for ADT drivers require an effective suspension seat to reduce the vibration exposure the driver is exposed to.

ADT drivers are exposed to high levels of whole body vibration. This is hazardous to their health and decreases daily operating efficiency. The general solution to this is the use of a suspension seat. There are a variety of suspension seats commercially available, all using the same scissor mechanism with steel springs; the more expensive seats use air-springs. In this project a new ADT suspension seat concept with vertical and lateral degrees of freedom was designed, built and tested.

Current suspension seats isolate vibration only in the vertically and fore-aft directions, but not laterally. Measurements have shown that the lateral vibration frequently exceeds the daily exposure limit according to the EU Directive 89/391/EEC. Thus a suspension seat isolating vibration within acceptable limits vertically and fore-aft, but not laterally will still expose the occupant to levels above the Directive's limit.

The suspension seat designed in this project isolated the vertical vibration input comparable to the best performing suspension seats, while at the same time also isolating the vibration in the lateral direction.

The new ADT suspension seat's vertical vibration isolation is comparable to the best performing commercial suspension seats. The seat does not make use of the commonly used scissor mechanism to dictate translation, but a new mechanism that can provide vertical and lateral translation. Each mechanism does have its advantages and disadvantages. Although for current seats to compete with the new

suspension seat, the current seats will have to be modified to be able to isolate lateral vibration.

- Good correlation was achieved between the numerical modelling and laboratory test data. The purpose of the numerical modelling was to aid in the generation of the system specifications. The models were not only used for analysis, but also as a design tool. Refinements were made to the models to obtain better correlation with the measured data. The improved models showed good correlation with the measured data and can be used in the development of suspension seats for other vehicles.
- A structured systems engineering design approach was used. A system engineering approach was used for the design and development of the suspension seat. The ADT cabin operating environment was analysed and compared with the customer requirements, to generate the system specifications. Concept generation included the generation of various concepts from the system specifications and evaluation relative to the customer requirements. The initially chosen concept was not feasible and the final concept chosen for prototype design and manufacture was also flawed. Through an iterative process the first prototype was refined to a functional system. System specifications and B-specifications were obtained with numerical modelling and the modelling was also used to successfully predict behaviour, evaluate and refine the new suspension seat. With the models the seat can also easily be adapted to be used in other vibration environments. This project did not finish with a detailed design, but only with the concept phase and a first working prototype. Enough information was obtained and the concept was proven satisfactory to justify another prototype. Another prototype will be necessary to fully prove the technology so as to enter the detail design and development phase.

It is recommended that a second, refined prototype be manufactured.

Another prototype was designed with information obtained from the first prototype's evaluation and testing. At the start of project there were many unknowns, as well as substantial design freedom. During the course of the project a better understanding of the problem was obtained. With this new information an improved design was developed. All the specifications of the next prototype have not yet been completely verified, but initial prediction seems promising.

References

Benham P.P., Crawford, R.J., Armstrong, C.G., 1996, Mechanics of Engineering Material, Second Edition. Prentice Hall.

Blanchard, S., Fabrycky, W.J., 1998, Systems Engineering and Analysis Third Edition. Prentice Hall International Series In Industrial and Systems Engineering.

Brereton, P., Nelson, C., 2004, Progress with implementing the EU Physical Agents (Vibration) Directive in the United Kingdom, 39th United Kingdom Group Meeting on Human Response to Vibration, 15-17 September 2004, pp 293-300, Ludlow England.

EU-Directive, 2002, Directive 2002/44/EC of European Parliament and of the council of June 2002, Official Journal of European Communities.

Greenberg, J.A., Jeyabalan, V.J., Meier R.C., and Pielemeier, W.J., 1998, The Dyanmic Characteristics of 16 Automibile seats. Ford Technical Report. Project No.: AJ452.

Griffin, M.J., 1990, Handbook of Human Vibration. Academic press limited.

Gunaselvam, A.J.M, 2004, The Use of Seating Systems to Reduce Whole Body Vibration Exposure in The SA Industry, MScEng (Mech) Thesis, University of Stellenbosch.

Gunston, T.P., Rebelle, J., Griffin, M.J., 2002, A comparison of two methods of simulating seat suspension dynamic performance, Elsevier, Journal of Sound and Vibration 278 (2004) 117–134.

Harsta, A., 2006, Horizontal Seat Suspension for Articulated Dump Trucks, MScEng (Mech) Thesis, Delft University of Technology.

Inman, J., 2001, Engineering Vibration Second Edition, Prentice Hall International, Inc., Upper Saddle River, New Jersey 07458.

International Organization for Standardization, 1990, Mechanical vibration and shock – Guidance on safety aspects of tests and experiments with people – Part 1: Exposure to whole-body mechanical vibration and repeated shock, ISO 13090-1.

International Organization for Standardization, 1992, Mechanical vibration – Laboratory method for evaluating vehicle seat vibration – Part 1: Basic requirements, ISO 10326-1.

International Organization for Standardization, 1997, Mechanical vibration and shock – Evaluation of human exposure to whole-body vibration – Part 1: General requirements, ISO 2631-1.

International Organization for Standardization, 2000, Earth-moving machinery – Laboratory evaluation of operator seat, ISO 7096.

International Organization for Standardization, 2004, Mechanical vibration and shock – Evaluation of human exposure to whole-body vibration – Part 5: Method for evaluation of vibration containing multiple shocks, ISO 2631-5.

Kirstein, J.C., 2005, Suspension System Optimisation to Reduce Whole Body Vibration Exposure on an Articulated Dump Truck, MScEng (Mech) Thesis, University of Stellenbosch.

Lewis C.H. and Griffen M.J., 1998. A comparison of evaluations and assessments obtained using alternative standards for predicting the hazards of repeated shock. Journal of Sound and Vibrations 215(4), 915-926, Article No. sv981591.

Mansfield, N.J., Lundström, R, 1999, Models of the apparent mass of the seated human body exposed to horizontal whole-body vibration, *Aviation, space, and environmental medicine*, 70(12):1166-72.

Matlab, 2007, Help Files, Version R2007b, Mathwork, Natick, Massachusetts, USA.

Perry, R.H., Green, D.W., 1984, *Perry's Chemical Engineers' Handbook*, Sixth Edition, McGraw Hill. ISBN 0-07-049479-7.

Seidel, H., Heide, R., 1986, Long-term effects of whole-body vibration a critical survey of the literature. *International archives of Occupational and Environmental Health* 58:1-26.

Ullman, G., 1997, *The Mechanical Design Process*, McGraw Hill International Editions.

US Army, Air Force, Navy, 1998, *Anthropometry and Mass Distribution for Human Analogues*, Volume I: Military Male Aviators, AARML-TR88-010, NAMRL-1334, NADC-88036-60, NBDL 87R003, USAFSAM-TR-88-6, USAARL 88-5.

van Niekerk, J.L., Heyns, P.S., Heyns, M., Hassall, J.R., 1998, Human vibration levels in the South African mining industry, 34th United Kingdom Meeting on Human Response to Vibration, Ford Motor Company, Dunton, Essex, 22nd to 24th September 1999.

Vesconite Specifications, [S.A.]. [Online], Available: <http://www.vesconite.com/charts/specs.htm#Vesconite%20-%20Specifications>, [2008, October 31].

Wu, X., Griffen, M.J., 1995, Towards The Standardization of Testing Method For The End-Stop Impacts of Suspension Seats, Academic Press Limited, Journal of Sound and Vibration (1996) 192(1), 307-319.

Wu, X., Rakheja, S., 1999, Dynamic Performance of Suspension Seats Under Vehicular Vibration and Shock Excitations, Society of Automotive Engineers, Inc, ISSN 0148-7191.

Wynand, C., 2004, Engineering Entrepreneurship, Steering Start-ups to Steady-State, Published and distributed by MW Coetzer.

Appendix A: Derivations

A.1 Air-spring

The generally used and standard method to calculate pressure losses over and mass flow through an orifice was used. With the up-stream high pressure P_1 and the downstream low pressure P_2 . During operation the pressure inside the air-spring and reservoir will change between the low and high pressure region. Figure A.1 shows the air flow through the orifice.

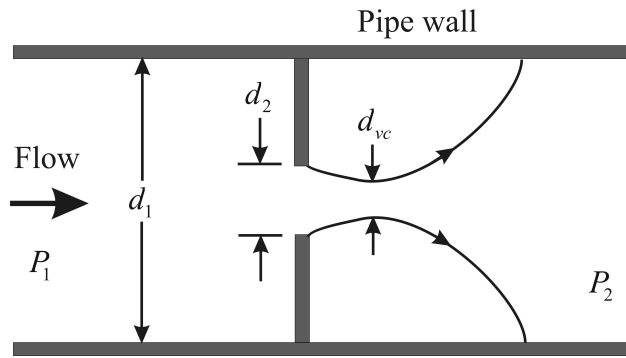


Figure A.1: Air flow through orifice

From the Bernoulli equation the relationship between pressure and velocity:

$$P_1 + \frac{1}{2} v_1^2 \rho = P_2 + \frac{1}{2} v_2^2 \rho \quad (\text{A.1.1})$$

with:

$$\Delta P = P_1 - P_2 \quad (\text{A.1.2})$$

$$Q = v_1 A_1 = v_2 A_2 \quad (\text{A.1.3})$$

Areas are calculated from the geometry of the pipe and orifice (with the same subscript):

$$A_1 = \frac{d_1^2 \pi}{4} \text{ and } A_2 = \frac{d_2^2 \pi}{4} \quad (\text{A.1.4}) \text{ and } (\text{A.1.5})$$

thus:

$$\Delta P = \frac{Q^2 \rho}{2A_2^2} \left(1 - \left(\frac{A_2}{A_1} \right)^2 \right) \quad (\text{A.1.6})$$

With the coefficient of discharge C_d , defining the orifice flow coefficient:

$$C = C_d \sqrt{\frac{1}{1 - \beta^4}} \quad (\text{A.1.7})$$

with:

$$\beta = \sqrt{\left(\frac{A_2}{A_1} \right)} \quad (\text{A.1.8})$$

Redefining equation 6.4 using equation 6.5:

$$Q = CA_2 \sqrt{\frac{2\Delta P}{\rho}} \quad (\text{A.1.9})$$

From Perry *et al.* (1984) the expansion factor is given by:

$$Y = \sqrt{r^{2/n} \left(\frac{n}{n-1} \right) \left(\frac{1 - w^{(n-1)/n}}{1 - w} \right) \left(\frac{1 - \beta^4}{1 - \beta^4 w^{2/n}} \right)} \quad (\text{A.1.10})$$

When $\beta < 0.25$ it is approximated by $\beta \approx 0$, thus:

$$Y = \sqrt{r^{2/n} \left(\frac{n}{n-1} \right) \left(\frac{1 - w^{(n-1)/n}}{1 - w} \right)} \quad (\text{A.1.11})$$

Inserting the expansion factor to the volumetric flow, equation 6.7:

$$Q = CA_2 Y \sqrt{\frac{2\Delta P}{\rho}} \quad (\text{A.1.12})$$

thus:

$$Q = CA_2 \sqrt{r^{2/n} \left(\frac{n}{n-1} \right) \left(\frac{1 - w^{(n-1)/n}}{1 - w} \right) \left(\frac{2\Delta P}{\rho} \right)} \quad (\text{A.1.13})$$

The density of air is calculated from the upstream pressure:

$$\rho = \frac{P_1}{RT} \quad (\text{A.1.14})$$

The mass flow through the orifice is given by:

$$\dot{m} = \rho Q \quad (\text{A.1.15})$$

Inserting equation 6.11 and 6.12 into equation 6.13 and solving:

$$\dot{m} = CA_2 P_1 \sqrt{\frac{2}{RT} \left(\frac{n}{n-1} \right) \left(w^{2/n} - w^{(n+1)/n} \right)} \quad (\text{A.1.16})$$

with:

$$w = \frac{P_2}{P_1} \quad (\text{A.1.17})$$

Ideal gas equation calculations

Volume change of air spring:

$$V_a = (L_{a0} + z_a - z_b) A_a \quad (\text{A.1.18})$$

$$\dot{V}_a = (\dot{z}_a - \dot{z}_b) A_a \quad (\text{A.1.19})$$

To use the mass flow rate through an orifice equation (equation 6.14), the time derivative of the ideal gas equation was used for the air spring and reservoir:

$$P_a V_a = mRT_a \quad (\text{A.1.20})$$

$$\frac{d}{dt}(P_a V_a) = \frac{d}{dt}(mRT_a) \quad (\text{A.1.21})$$

According to the chain rule:

$$\dot{P}_a V_a + \dot{V}_a P_a = \dot{m} R T_a \quad (\text{A.1.22})$$

This is then solved for the partial pressure of the air:

$$\dot{P}_a = \frac{\dot{m} R T_a - \dot{V}_a P_a}{V_a} \quad (\text{A.1.23})$$

For the reservoir:

$$P_r V_r = m_r R T_r \quad (\text{A.1.24})$$

$$\frac{d}{dt}(P_r V_r) = \frac{d}{dt}(m_r R T_r) \quad (\text{A.1.25})$$

with $V_r = \text{constant}$ then:

$$\dot{P}_r V_r = \dot{m} R T_r \quad (\text{A.1.26})$$

solving:

$$\dot{P}_r = \frac{\dot{m} R T_r}{V_r} \quad (\text{A.1.27})$$

The pressure difference between air spring and reservoir determines the flow direction. The higher pressure is always used for the upstream pressure in equation 6.14.

For $P_a \geq P_r$:

$$P_a = P_1 \quad (\text{A.1.28})$$

$$P_r = P_2 \quad (\text{A.1.29})$$

$$w = \frac{P_r}{P_a} \quad (\text{A.1.30})$$

For $P_a < P_r$:

$$P_a = P_2 \quad (\text{A.1.31})$$

$$P_r = P_1 \quad (\text{A.1.32})$$

$$w = \frac{P_a}{P_r} \quad (\text{A.1.33})$$

The initial pressure in the air spring and reservoir is given by:

$$P_{a0} = P_{r0} = \frac{M_a g}{A_a} + P_{atm} \quad (\text{A.1.34})$$

The force exerted by the air spring is given by:

$$F_s = (P_{atm} - P_a) A_a \quad (\text{A.1.35})$$

Equations A.1.16, A.1.23, A.1.27 and A.1.35 were solved numerically using Matlab Simulink.

A.2 ISO 7096 (2000) EM1 signal generation

A time dependant signal had to be generated as base input for laboratory testing and the numerical model. Only after the EM1 signal was generated was it realised that the available laboratory equipment could not achieve the vertical displacement. Before this was realised though, the objective was to write a Matlab code that would generate a time dependant signal. For laboratory testing the signal would have to be given as displacement and acceleration for the numerical modelling. The actuator input must be given as displacement. Using acceleration for the numerical model's input greatly reduces the numerical errors. A bias error does occur, but does not influence the results of the model. All the lumped masses experience the same bias error and what is of interest is the motion of the lumped masses relative to each other. Not its displacement to a fixed reference co-ordinate system. The standard method to generate a required frequency dependant signal is to use a random signal and filter it. The author did not approve of this method and decided to try something new a simple. A method to generate a displacement and acceleration signal from a required PSD. The method used might already be well established in literature. Because the signal generation is not a great focus point of the project it was not thoroughly searched after.

A function cr8_PSD.m was written in Matlab. The function loads a data file containing the required PSD and generates a displacement, velocity and acceleration time dependant signal.

The run function expression:

`[t_out y_out] = cr8_PSD(f_res,dt,tend,order,gen_file)`

`f_res (Δf)` : Period of the PSD input signal.
`dt (Δt)` : Required period of the time output signal
`tend (t_{end})` : End time of output signal
`order (j)` : Time derivative of the output signal. The function can give displacement, velocity and acceleration, but to save memory for use in the numerical simulation the order of the output can be defined as input.
`gen_file` : The name of the file containing the required PSD.

The time output is given by:

$$t = 0 : \Delta t : t_{end} \quad (A.2.1)$$

$G_{ss}(t)$ is the required PSD input loaded from the input file. The number of iterations (N) required to generate the signals is dependent on the period of the frequency (Δf) and the frequency end value (f_{end}):

$$N = \frac{f_{end}}{\Delta f} \quad (A.2.2)$$

The phase angle θ_n was randomly generated for each frequency component between $\pm\pi$. The Matlab function `randn` was used which gives normally distributed random numbers (Matlab help, 2007) as output.

The amplitude at each frequency component was calculated from the PSD amplitude input:

$$B_i = \sqrt{G_{ss_i} \Delta f} \quad (A.2.3)$$

The PSD input is of the required acceleration and thus the acceleration was used and integrated to obtain the velocity and displacement. The acceleration time dependant signal:

$$y = \sum_{i=1}^N [B_i \sin(2f_i \pi t_i + \theta_i)] \quad (\text{A.2.4})$$

The velocity time dependant signal:

$$\int_0^{t_{end}} y dt = \sum_{i=1}^N \left[-\frac{B_i \cos(2f_i \pi t_i + \theta_i)}{2f_i \pi} \right] \quad (\text{A.2.5})$$

The displacement time dependant signal:

$$\int_0^{t_{end}} \int_0^{t_{end}} y dt dt = \sum_{i=1}^N \left[-\frac{B_i \sin(2f_i \pi t_i + \theta_i)}{(2f_i \pi)^2} \right] \quad (\text{A.2.6})$$

The period at which the signal repeats itself (H) is dependent on the period of the frequency response:

$$H = \frac{1}{\Delta f} \quad (\text{A.2.7})$$

Appendix B: CAD renders



Figure B.1: 3-D drawings of first prototype suspension seat



Figure B.2: 3-D drawings of lateral test setup

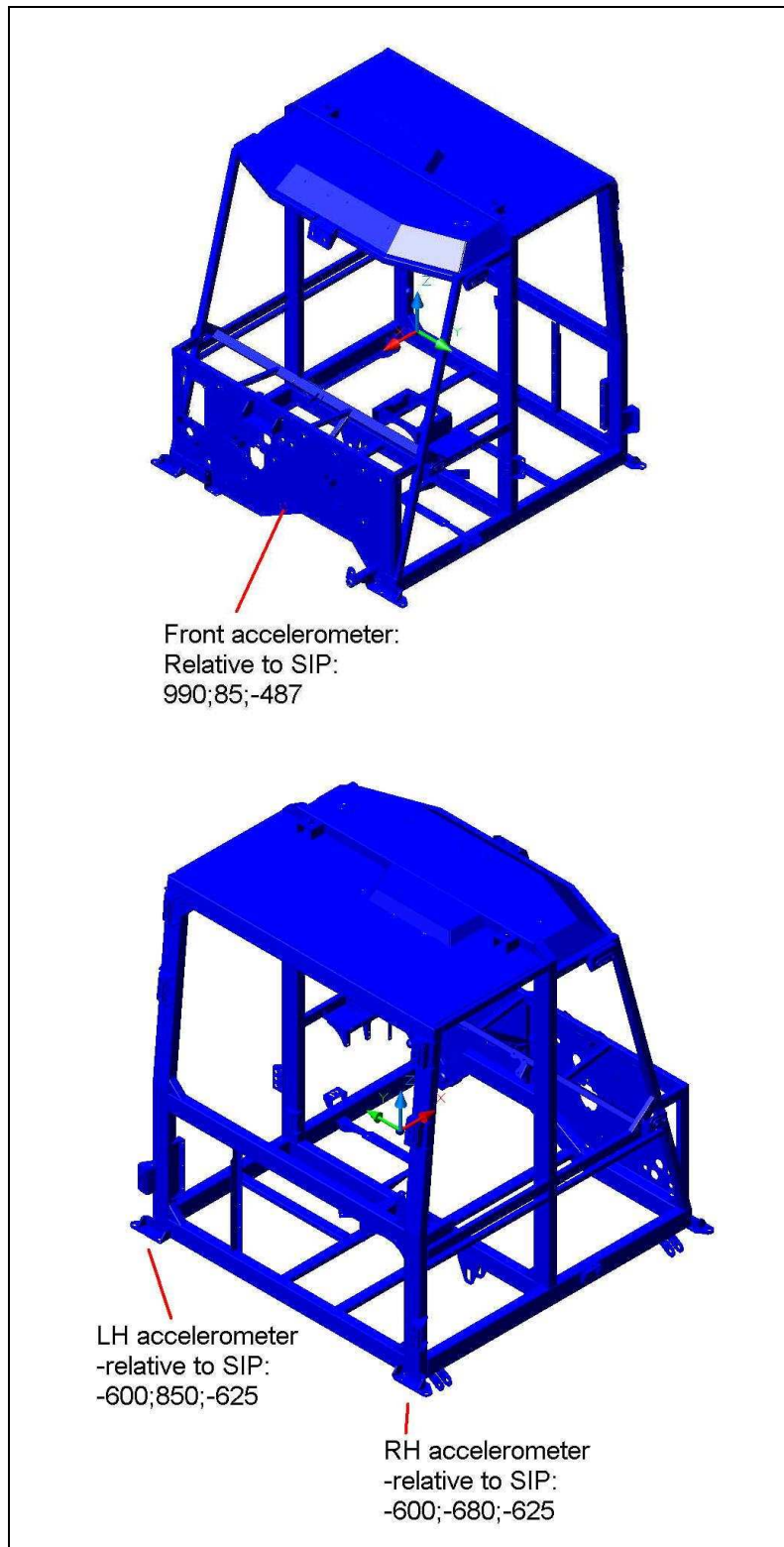


Figure B.3: 3-D drawing of accelerometers positions in ADT cabin

Figure B.4 shows a drawing of the Rosta unit. It consists of an outer housing and an inner square shaft that is supported with interference fitted rubbers. When the inner square shaft rotates relative to the outer housing it compresses the rubber. This mechanical behavior then supplies the Rosta's angular stiffness.

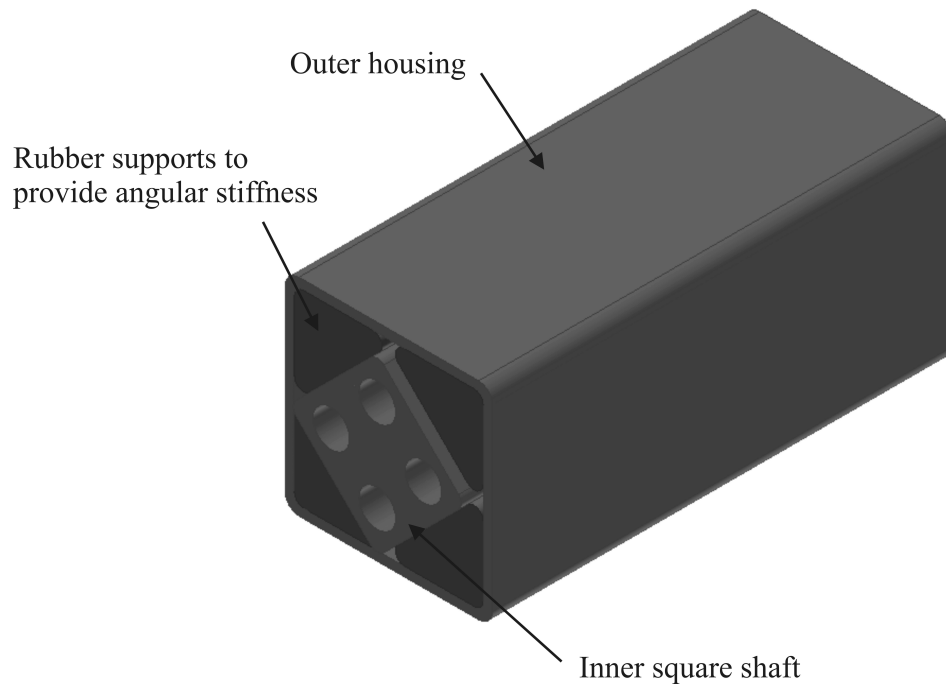


Figure B.4: 3-D drawing of Rosta unit

Appendix C: ADAMS models

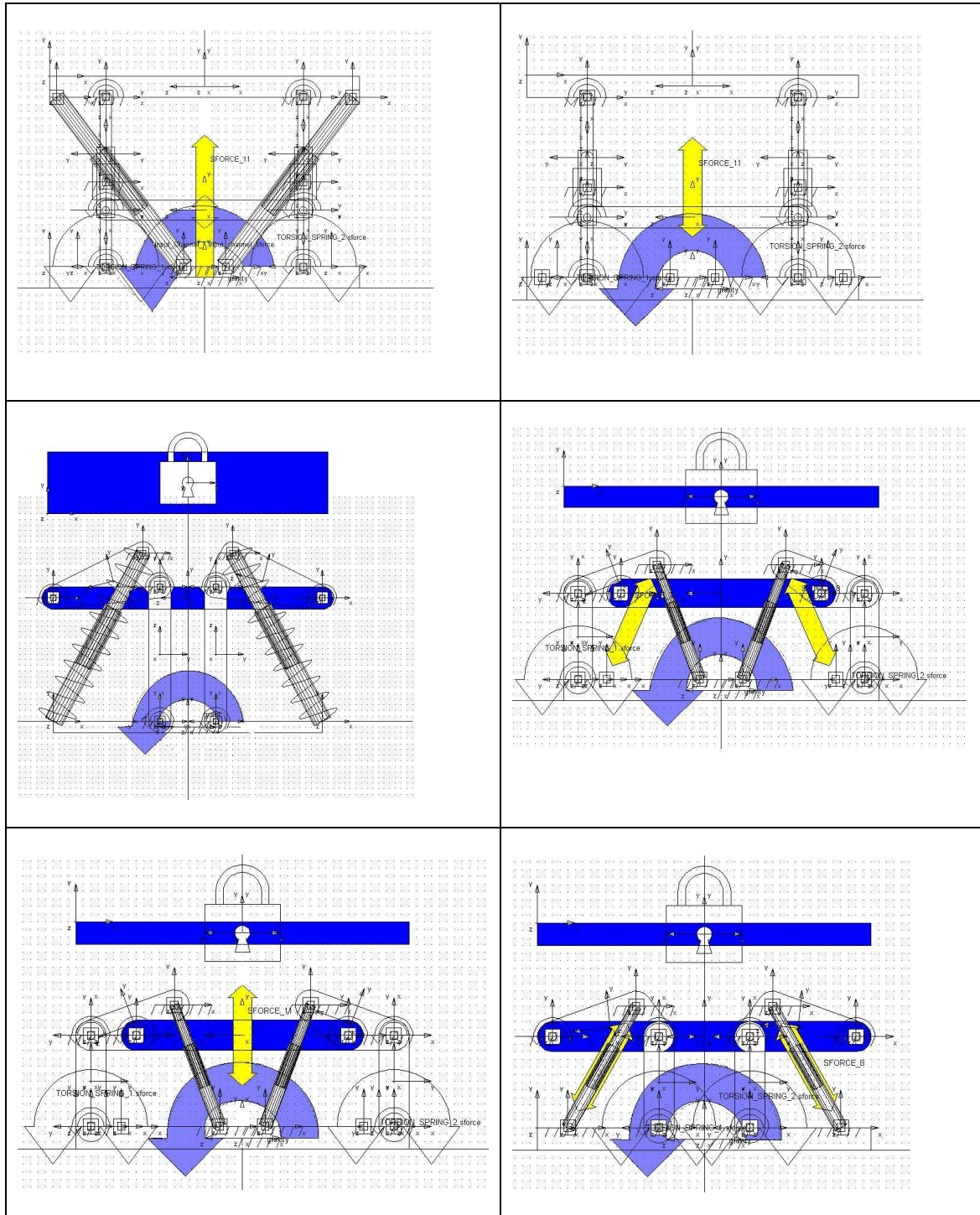
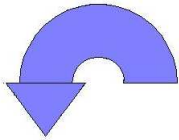
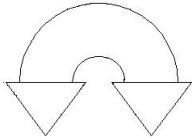
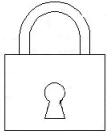
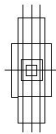

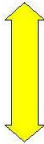
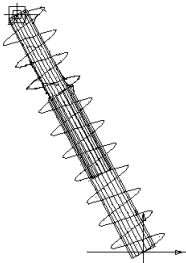


Figure C.1: ADAMS models created in the suspension seat concept phase

Figure C.1 continued: Legend

	
Base displacement. Translation and rotation	Angular spring
	
Locking element between two elements	Slider mechanism
	
Pivot point between two elements	Basic air-spring model
	
Linear spring and damper	